Additive Manufacturing 74 (2023) 103728

Contents lists available at ScienceDirect

Additive Manufacturing

journal homepage: www.elsevier.com/locate/addma

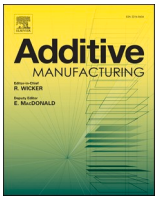

Design optimization of hot stamping tooling produced by additive manufacturing

Dimitrios Chantzis [a], Michaela Tracy [a], Heli Liu [a], Denis J. Politis [b], M.W. Fu [c], Liliang Wang [a,*]

[a] Department of Mechanical Engineering, Imperial College London, Exhibition Road, London SW7 2AZ, UK
[b] Department of Mechanical and Manufacturing Engineering, University of Cyprus, Nicosia 1678, Cyprus
[c] Department of Mechanical Engineering, Research Institute for Advanced Manufacturing, The Hong Kong Polytechnic University, Hung Hom, Kowloon, Hong Kong, Special Administrative Region

ARTICLE INFO

Keywords:
Lattice Structure
Hot Stamping
Hot Stamping Tooling
Additive Manufacturing
Design Optimization

ABSTRACT

The design flexibility of Additive Manufacturing (AM) can be utilized to develop innovative and sustainable hot stamping tools with enhanced quenching capability compared to tools manufactured by conventional manufacturing processes. This study proposes a concept for hot stamping tools with integrated lattice structures that selectively substitute a die's solid areas. A lattice structure demonstrates reduced thermal mass and can affect the ability of the tool to absorb heat from the blank and the rate at which the tool is cooled between two consecutive stamping cycles. This study explores the design space of a hot stamping tool with integrated lattice structures. It presents the optimized design for an effective compromise between cooling performance, structural integrity, and several other design parameters shown in the study. The proposed method utilizes a 2D thermo-mechanical finite element analysis model of a single cooling channel combined with Design of Experiments (DoE) to reduce the computational cost. The results show that the integration of lattice structure cannot only deliver improved cooling performance with minimum change in the dimensions of the cooling system but also achieves a faster AM build time since less material is required to be printed.

1. Introduction

Electrification and sustainable manufacturing are being adopted at an increasing rate by the automotive industry, with the EU advising the termination of sales of internal combustion vehicles by 2035[1]. These trends are driven by stricter vehicle emission regulations and international agreements that envisage tackling climate change. Moreover, the development and production of battery electric vehicles (BEV) add further pressure to the already small margins of automotive OEMs because they must preserve the current production of internal combustion engine (ICE) vehicles until the transition to electrification is completed. As a result, automotive OEMs respond to these challenges by focusing on cost efficiency, allowing them to free necessary capital to finance current and future vehicle programs.

A lightweight design approach is significant for OEMs since weight affects both the cost and emissions for internal combustion engine (ICE) vehicles or the range of a battery electric vehicle (BEV). Although several lightweight design paradigms have been proposed in the last decades, high-volume OEMs have focussed on steel Body in White (BiW) [2] and some cases, aluminum [3,4] as the areas of most significant impact. The reason is that OEMs have extensive knowledge regarding the formability of steel grades and their performance during impact crash events. At the same time, in the case of aluminum, there is significant potential in the improved strength-to-weight ratio compared to other materials, especially in multi-loading cases of compoenents, as well as unique corrosion behavior. Advanced steel and aluminum alloys such as ultra-high-strength steel (UHSS) or AA7075-T6 are some of the materials used in safety-critical areas of the BiW, such as roof rails [5], door impact beams [6] and B-pillar inner [7,8] components. However, due to their poor formability, these advanced alloys cannot be formed into complex-shaped components at room temperature. To overcome this issue, the hot stamping process is widely adopted by automotive manufacturers and suppliers [9]. During hot stamping, the temperature of the blank is increased. This can be achieved by various methods, usually by convection with a furnace or, in other cases, with contact, resistance, or induction heating. When the blank reaches the desired temperature, it is then transferred to the dies so it can be formed and quenched [10]. The tool design is significantly complex with internal channels where

* Corresponding author.
E-mail address: liliang.wang@imperial.ac.uk (L. Wang).

https://doi.org/10.1016/j.addma.2023.103728
Received 6 April 2023; Received in revised form 1 August 2023; Accepted 5 August 2023
Available online 7 August 2023

water is circulated inside the tool to quench the blank at a specific cooling rate. The required rate varies across different materials from 27 °C/s for Boron Steel [11] to 100 °C/s for AA7065 [12] and the thermo-mechanical properties of the final product can be susceptible to this value. In general, hot stamping is a sophisticated forming process that the thermo-mechanical process parameters must be controlled with high precision and the importance of tooling must be highlighted.

Besides the engineering challenges in developing hot stamping tools, another aspect that should be considered is cost. Although hot stamping is a process that produces components of high geometric complexity, a single change in the geometry of the component could make the die redundant. This is the reason why the use of hot stamping is a strategic decision and is taken based on a cost-benefit analysis. For instance, many OEMs select UHS steel for the B-Pillar[13], a safety-critical component that enables safety requirements to be met with a light-weight and low gauge structure. Moreover, tooling cost is a crucial driver for the automotive industry to develop modular platforms since it is more cost-effective when the cost of a die is amortized over greater volumes.

The current manufacturing practice is to produce hot stamping dies by subtractive processes leading to a high "buy to fly" ratio, increasing the manufacturing waste and material cost. Another technical disadvantage of the conventional manufacturing process is that it cannot effectively produce cooling channels that can follow the tool's geometry to demonstrate better quenching performance. Several studies have proposed different manufacturing strategies to overcome this issue such as fabricating two-piece die, usually an upper and a lower one, with the cooling channels divided between them [14], casting dies with pre-fixed formed tubes in the mould [15] or segmenting the die into numerous "segments" to allow for the drilling of conformal cooling channels [16]. Although all these approaches provide higher design flexibility to the tool each method is a balance between the advantages offered and the disadvantages e.g. segmenting a die is possible but issues with alignment and time required to complete the process may offset the benefits. As far as the engineering development of a hot stamping die is concerned, numerous studies focus mainly on designing and optimizing the cooling system. Chantzis et al.[17] published a comprehensive review on hot stamping tooling design. A considerable number of studies focus on identifying the main design variables of the hot stamping die's cooling system: cooling channel diameter and distance between two cooling channels. The analytical and computational modelling approaches are mainly followed since experimental studies are deemed rather costly, especially when there are numerous combinations of the cooling system's main design variables. Analytical models, which are mainly based on the energy conservation principle, provide a fast and reasonably accurate calculation of the basic dimensions of the cooling system. The accuracy can be radically improved using computational models, but they are computationally intensive. Some new methods try to decrease the computational time by first segmenting the die geometry into areas of specific geometric characteristics such as radii, flat areas, and chamfers. Finally, the die's performance is evaluated using the data from each segment after analyzing each geometry characteristic individually. Such methods can reduce the model solving time by 92% without compromising accuracy[18].

Additive Manufacturing (AM) is an innovative technology that enables the manufacturing of intricate and optimized parts without the component's complexity significantly affecting its cost. Using AM technologies, engineers have managed to manufacture topology-optimized components minimizing their weight while maximizing their performance. Studies have shown applications with significant improvement from structural and heat transfer points of view using design optimization. Despite the design flexibility and the obvious associated performance benefits, AM technologies suffer from low deposition rates, and currently, this is the main barrier to adoption from high-volume industries. However, this is not the case for hot stamping dies since they are low-volume applications with production cycle times of the order of 25 weeks on average [19]. The research community has identified the potential of AM for this application, and studies show that sophisticated tools with significantly improved quenching performance are feasible. This is essential as cooling performance is directly related to the processing time. Moreover, an inherent benefit of AM is that the buy-to-fly ratio is almost 1 improving manufacturing sustainability.

Cortina et al. [20]used additive manufacturing to produce a hot stamping die with conformal cooling channels. The tool was fabricated by the Laser Metal Deposition (LMD) technology and subsequently milled to attain the final geometry. The test specimens were evaluated and compared to traditional straight-cut channels demonstrating equivalent performance, showing that LMD, which can be used to manufacture conformal cooling channels cost-efficiently, can be an alternative manufacturing method for hot stamping dies. Muller et al. [21] used SLM to build a hot stamping die from steel 1.2709 with CC channels. In the proposed AM design, small diameter cooling channels were positioned closer to the blank-die interface, allowing the holding time to be reduced by 45%, from 11 s to 6, while delivering a more homogeneous temperature distribution within the blank. Moreover, AM technologies can enable the manufacturing of dies with integrated lattice structures with significant benefits for the hot stamping process. First, tailored thermal conductivity distributions can be achieved within the die by selectively substituting solid areas with lattice structures. Thus, the conduction of heat within the die through a guided path can be achieved, leading to more efficient heat dissipation by the cooling channel. In addition, lattice structures have lower thermal mass than their solid counterparts. Consequently, a die with integrated lattice structures can cool down faster than a conventional one between two consecutive process cycles. Lastly, the use of lattice structures is associated with lower printing requirements such as less time and material. Au and Yu [22,23] presented the idea of porous structures integrated into a mold with a constant distance from the working surface along its profile. Brooks and Brigden [24] showed that support lattices within the cooling channels might increase cooling performance as the lattices create a turbulent flow of water inside the channel increasing heat transfer. Recently, Chantzis et al.[25] proposed a method for designing hot stamping dies produced by Selective Laser Melting. Moreover, a strategy for integrating lattice structure into a die was proposed, which significantly increased the cooling performance to almost double and reduced the printing time by at least 12% compared to a traditional fully solid die.

While most studies focus on the development of hot stamping tools with conformal cooling channels and their associated benefits, this study aims to present a new approach to designing hot stamping tools. It leverages the design flexibility offered by additive manufacturing (AM) to strategically integrate lattice structures into the hot stamping die. The goal is to enhance its cooling performance and minimize the amount of material required for printing. A systematic approach is used to identify the optimum combination of several design variables, such as the cooling channel's radius, the distance from the working surface, the amount of lattice structure, and the thickness of the lattice struts. By changing the volume and type of the lattice structure, the thermal mass of the tool can be modified. In simple terms, a stamping tool with a large thermal mass can store heat, making the quenching step of hot stamping more efficient, especially in the first few forming cycles. However, after several cycles, the tool's temperature converges at relatively high levels, which reduces the efficiency of the quenching. This study aims to identify the optimum thermal mass of the tool to maximize quenching performance for aluminum forming without, at any point, the stress levels of the tool being higher than its yield strength. The thermal mass of the tool will be altered by different levels of lattice structure integration in the hot stamping tool.

The paper is organised as follows. The proposed thermo-mechanical optimization workflow is described in Section 2 with the design variables, design of experiments strategy, and evaluation criteria being defined as well. In Section 3, the thermo-mechanical modelling of a hot

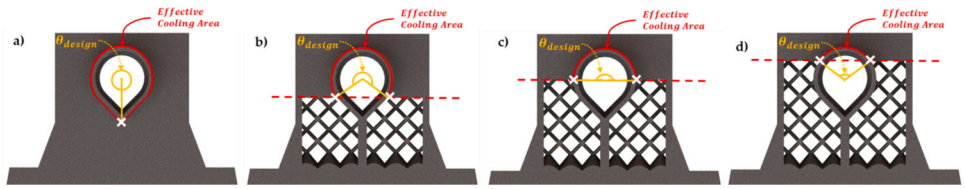

Fig. 1. Graphical Representation of lattice structure integration strategy [25].

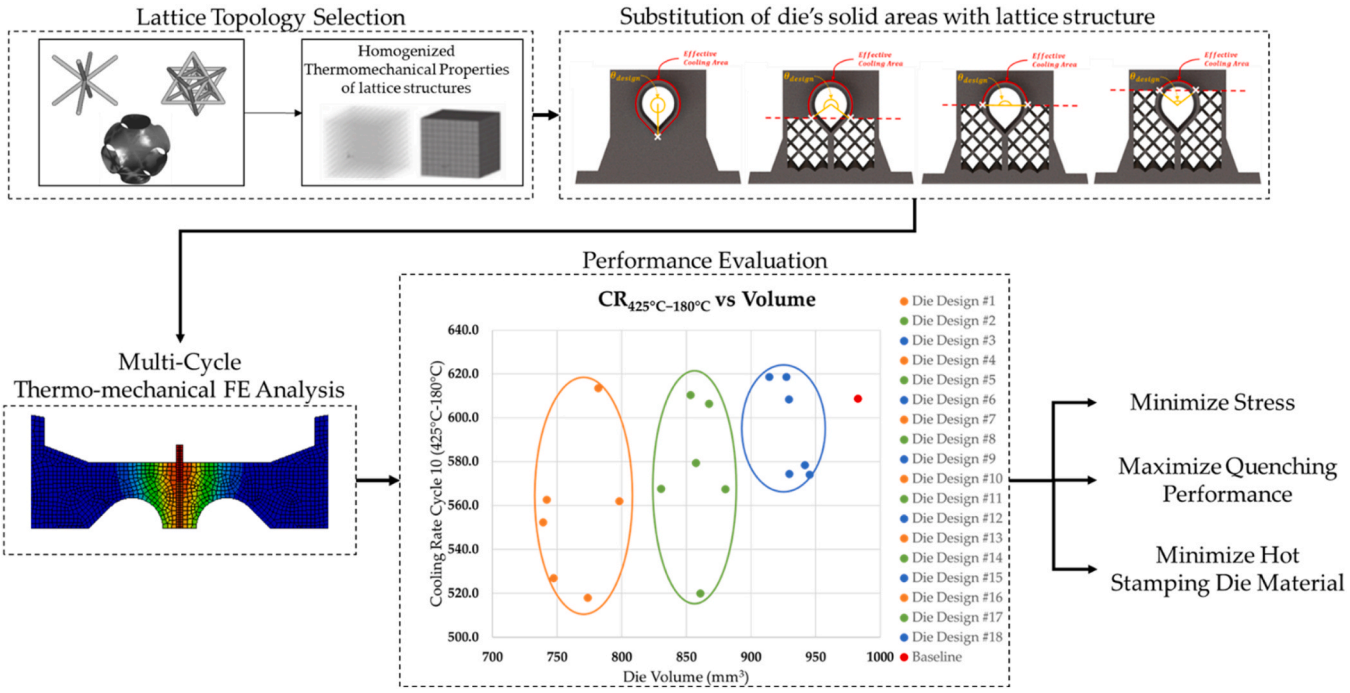

Fig. 2. Overview of the Proposed Design Optimisation Workflow.

Table 1
Design Variables and their respective values.

Factor	Level 1	Level 2	Level 3
Lattice type (A)	BCC	Octet-truss	Schoen IWP
Lattice density (B)	10%	50%	80%
Lattice amount (C)	120°	180°	270°
Cooling channel radius (D)	3 mm	4 mm	5 mm
Distance to working surface (E)	6 mm	7 mm	8 mm

stamping die is presented, along with the part geometry, the lattice structure types used in this study and their homogenized thermo-mechanical properties. In Section 4, the optimization results are presented, while in Section 5 and Section 6, the results are discussed, and conclusions are drawn, respectively.

2. Method

2.1. Proposed workflow

The proposed design workflow consists of 3 steps, i.e., design variable selection, design space exploration, and performance evaluation. In the design variables selection, the user initially selects a lattice topology that will be integrated into the die's body. All available lattice structures should be evaluated for manufacturability from AM, specifically powder bed laser fusion processes. For instance, a Body Centred Cubic (BCC) lattice is available when the angle of the strut to the building direction is greater than 45° to enable self-support printing. Subsequently, the lattice cell homogenization is performed to obtain the effective density, Poisson ratio, Young's modulus, and thermal conductivity. After obtaining the lattice cell's effective material properties, the dies' solid areas are selected to be substituted with lattice structures. The amount of lattice structures is controlled by the θ_{design} angle, which essentially represents the effective cooling area of the cooling channel (Fig. 1). The concept of the θ_{design} angle is explained in the publication of Chantzis et al.[25].

During the design exploration phase, different die designs with different design variables values are simulated with a multi-cycle 2D thermo-mechanical FEA model developed in ABAQUS. The quenching rate of the blank and the volume of the die are stored for processing at a later stage. As there is no upper limit to the combinations of design variables, a Design of Experiments (DoE) methodology is used to investigate the trade space between the die's response and the selected design variables. In the performance evaluation step, statistical analysis and linear interpolation models are presented to select the optimum die design in terms of thermal response and minimum material (Fig. 2).

2.2. Design of Experiments

A Design of Experiments (DoE) methodology was employed to explore the trade space of the proposed design approach for hot stamping dies. The Taguchi orthogonal array was utilized to examine the impact of various factors, including lattice type (L.T.), lattice density (L.D.), lattice amount (L.A.), and cooling channel radius (CD). The design variables, corresponding levels, and virtual runs are presented in Table 1 and Table 2, respectively. Each run represents a distinct die design

Table 2
Virtual runs for design space exploration.

Die Design	Lattice Type (A)	Lattice Density (B)	Lattice Amount (C)	Channel Radius (D)	Distance to Working Surface (E)
1	BCC	10%	120°	3 mm	6 mm
2	BCC	50%	180°	4 mm	7 mm
3	BCC	80%	270°	5 mm	8 mm
4	Octet Truss	10%	120°	4 mm	7 mm
5	Octet Truss	50%	180°	5 mm	8 mm
6	Octet Truss	80%	270°	3 mm	6 mm
7	Schöen-IWP	10%	180°	3 mm	8 mm
8	Schöen-IWP	50%	270°	4 mm	6 mm
9	Schöen-IWP	80%	120°	5 mm	7 mm
10	BCC	10%	270°	5 mm	7 mm
11	BCC	50%	120°	3 mm	8 mm
12	BCC	80%	180°	4 mm	6 mm
13	Octet Truss	10%	180°	5 mm	6 mm
14	Octet Truss	50%	270°	3 mm	7 mm
15	Octet Truss	80%	120°	4 mm	8 mm
16	Schöen-IWP	10%	270°	4 mm	8 mm
17	Schöen-IWP	50%	120°	5 mm	6 mm
18	Schöen-IWP	80%	180 °	3 mm	7 mm

employed to simulate a 10-cycle hot stamping process. The lattice type values can be varied between Body Centered Cubic (BCC), Octet-Truss, and Schoen IWP, whereby the first two constitute strut-based lattices, while the latter corresponds to a TPMS type. The suitability of these lattice types was assessed from a manufacturability standpoint, as elaborated in Section 3.2. Lattice density denotes the percentage of the fully dense volume of a lattice unit, while lattice amount controls the extent of the die area replaced by lattices, as determined by the θ_{design} angle, as explained in Section 2.1.

2.3. Evaluation criteria

The study focuses on the geometry of the forming tool and the cooling performance benefits that can be leveraged from the integration of lattice structures independent of the die's material to quantify the thermal performance as well as the structural integrity of the die. As a result, 3 quantitative evaluation criteria are defined and 2 of them are blank-centric while the other one is die-centric. The reason for defining blank-centric criteria in addition to die-centric ones is that the final product of hot stamping is a component and its properties are directly related to its cooling rate during the process. Consequently, the evaluation criteria described below, focus on the quenching rate of the blank, which affects the blank's microstructure, and the maximum stress on the tool as an indicator of the tool's structural integrity.

- **Critical Cooling Rate between 425 ℃ and 180 ℃ ($CR_{425°C-180°C}$):** This evaluation criterion relates to the blank's microstructure. Different materials must be quenched at a minimum cooling rate to demonstrate sufficient post-form material properties. In the case of AA7075, the selected blank material in this study, the critical cooling rate is identified at 100 ℃/s [12] in the temperature interval between 425 ℃ and 180 ℃. Thus, after each cycle the dies must demonstrate a quenching capability higher than this rate. In the case that the cooling rate is not achieved, then degradation of mechanical properties of the final component is implied.
- **Productivity:** Productivity is a crucial aspect of the tool design process. In this study, the hypothesis is that a hot stamping tool with lower thermal mass would be able to cool down faster between two consecutive stamping cycles and operate at a lower temperature range during quenching, acting as a more efficient heat sink for the hot blank. The lower thermal mass can be achieved by substituting solid areas in the die with lattice structures. The effect of the proposed design can be

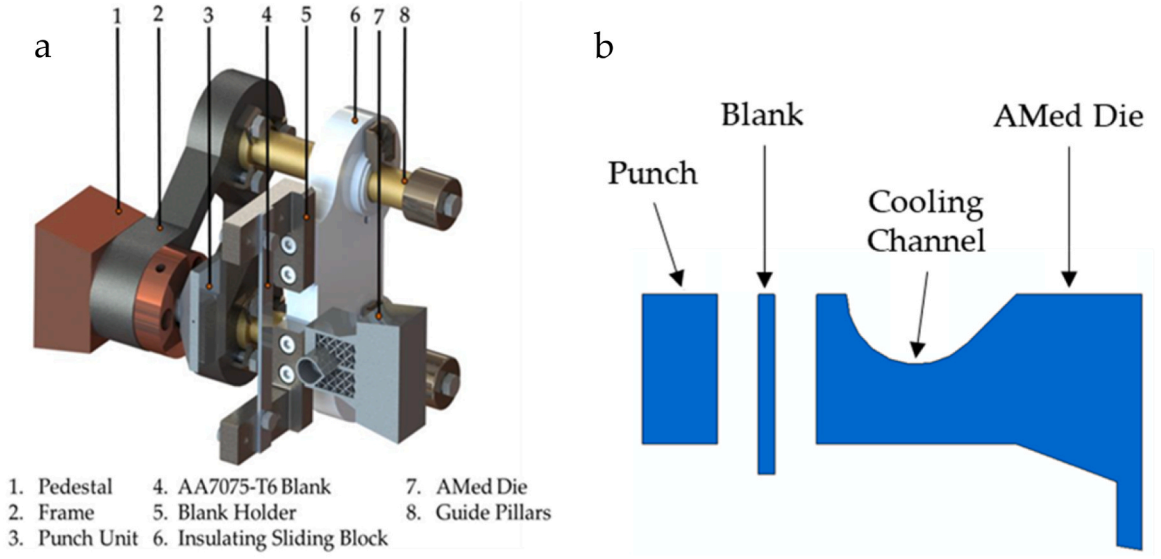

Fig. 3. (a)Experimental set up [28] and (b) 2D Thermo-mechanical model.

Table 3
Material Properties of the die and the blank.

	SS316	A7075
Density (g/cm3)	7.80	2.81
Young's modulus (GPa)	215	71.7
Poisson's ratio	0.27	0.33
Specific heat (J/kg°C)	500	960
Thermal conductivity (W/m-K)	17	130

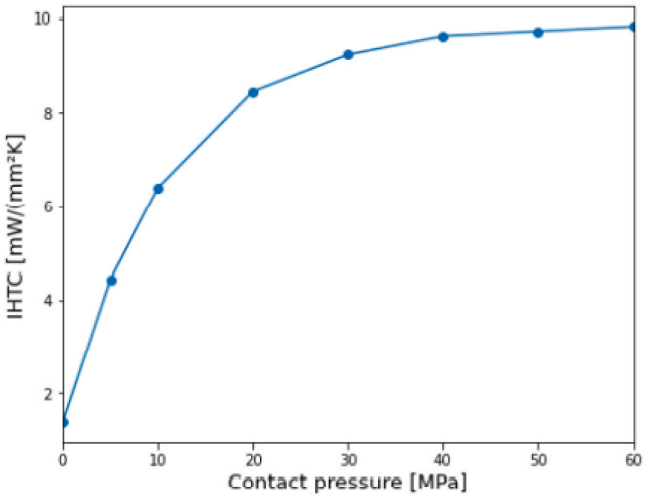

Fig. 4. Evolution of IHTC with the increase of contact pressure for SS-316 and AA7075 material combination [29].

quantified by calculating the cooling rate between 450 and 100 ℃ ($CR_{450°C-100°C}$). This temperature interval was selected based on the assumption that the blank must be lower than 100 ℃ due to artificial aging [26].

- **Maximum Stress:** In this study, the material selected for the die was stainless steel (SS) 316 with a yield strength of 498 MPa [27]. All the investigated designs should experience stresses below this value to maintain the structural integrity of the die during the operation.

3. Hot stamping modelling

3.1. 2D thermomechanical model development

The experimental data from the study by Chantzis et al. [25] were used to develop a 2D thermo-mechanically coupled hot stamping in ABAQUS. A single-cycle simulation of hot stamping was used to identify the key parameters of the FEA model, such as mesh size and boundary conditions, which will be used for the simulations outlined in Table 2. The experimental setup is presented in Fig. 3a along with the FEA model in Fig. 3b. The simulation consists of a single forming-quenching cycle, in which both the AMed die and the punch move towards the blank at a prescribed speed, a quenching stage in which the blank is held between the punch and the AMed die for a total of 5 s and a retraction stage in which the punch and the die return to their original position for 10 s until the blank is heated again to 450 ℃ for the next cycle. The blank transfer time is 0.5 s while the contact pressure is set at 15 MPa. The total simulation time of a single cycle is 5.5 s

At the start of the forming cycle, a uniform temperature of 25 °C assigned to the punch the AMed die. The fluid interactions within the cooling channel of the die are represented by a surface film condition with a constant surface film coefficient of 3 W/mm^2 °C that applies to the inner walls of the cooling channel. The temperature of the water in the cooling channel is set at 25 °C and remains constant throughout the whole simulation. The assumption of the constant surface film coefficient and water temperature is reasonable because of the simple geometry of the cooling channel and its short length. Other boundary conditions involve conduction heat losses from the blank to the punch. The conduction heat loss is driven by the Interface Heat Transfer Coefficient (IHTC) which is material and pressure dependent. In this study, the material of the punch and AMed die is stainless steel 316 (SS-316) and the blank is Aluminium T-7075 and their material properties are presented in Table 3.

While H13 and HTCS are generally considered more suitable materials for hot stamping tooling applications [17], SS316 was chosen for prototyping due to its availability and ease of handling. This study focuses on the die's design and its associated cooling performance improvement, as shown below. It is essential to note that the benefits demonstrated in this study are independent of the material choice, as they primarily stem from the integration of lattice structures into the die's body. The values for the IHTC between AA7075 blank and SS316 tool are shown in Fig. 4 and have been generated by a model-driven functional module, IHTC-Mate. IHTC-Mate was developed to predict the IHTC as a function of contact pressure for several blank-tool material

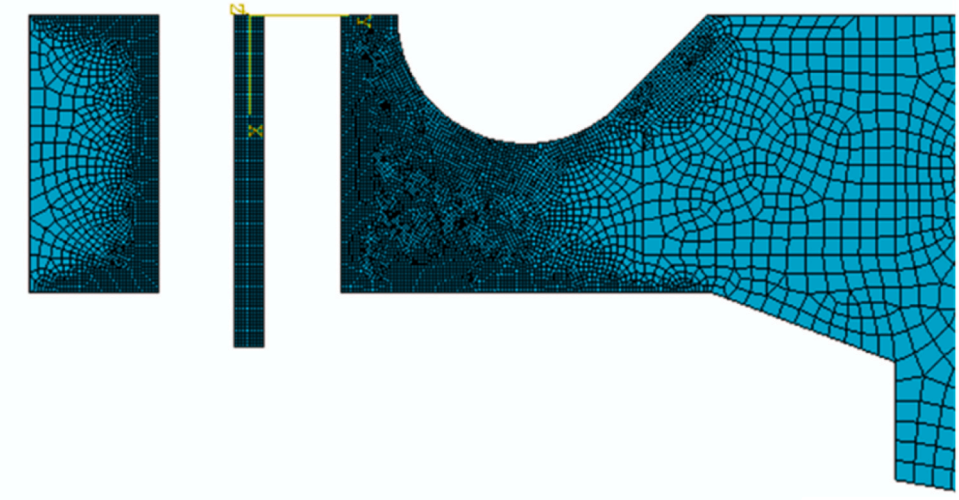

Fig. 5. Mesh representation of the validation model.

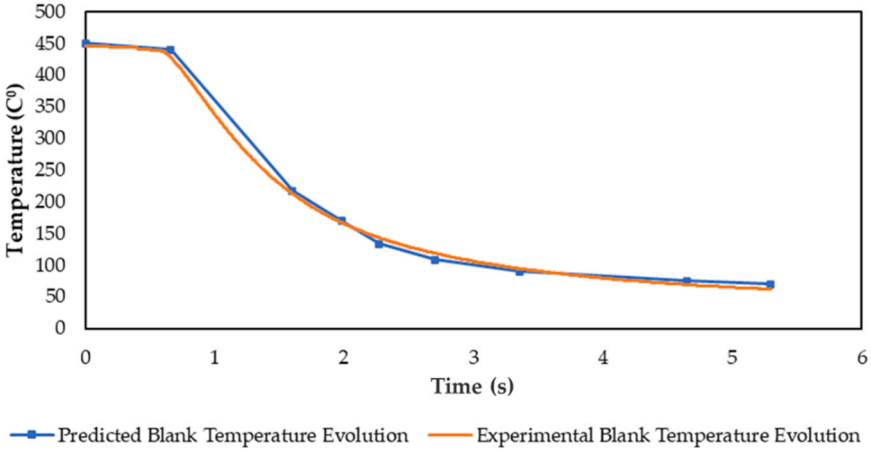

Fig. 6. Blank Temperature Evolution – Experimental data (Chantzis et al.[25]) vs Simulation.

Table 4
Selection of lattice structure for hot stamping tooling application.

Strut-Based		TPMS
BCC	Octet-truss	Schöen-IWP
		

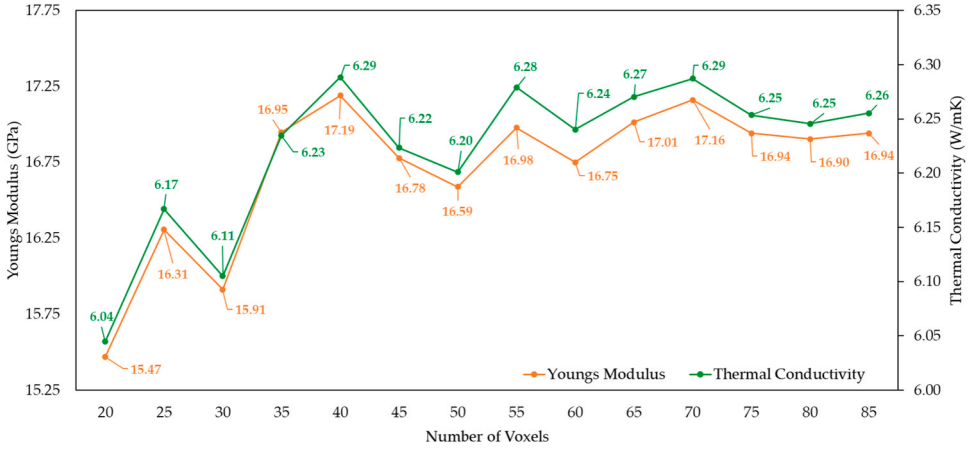

Fig. 7. Convergence study on the number of voxels for lattice structure homogenization.

combinations to enable FEA of hot stamping processes [29].

As far as the pre-processing of the FEA is concerned, the model meshed with a CPE4T element type, which is a thermally coupled quadrilateral element and the mesh size varies from 0.2 to 1.2 mm (Fig. 5). The blank, which is 2 mm is meshed uniformly with a constant 0.2 mm mesh size, while the mesh of the punch and the AMed die is denser towards their working surface, closer to the blank, and coarser towards their base. Total length.

A comparison between simulated and experimentally obtained blank cooling curves for a fully solid die is shown in Fig. 6. The exit temperature of the blank is predicted at 70 ℃ and shows good agreement with the respective experimental value, which is 62 ℃. Moreover, the model captures the blank temperature evolution in the temperature interval between 425 ℃ and 180 ℃, which is one of the evaluation criteria in this study. Specifically, the temperature standard deviation between experimental and simulated data, across the whole cycle, is 2.8 ℃ which shows that the FEA model parameters provide good accuracy and can be used for the multi-cycle hot stamping simulations of this study.

3.2. Lattice structure homogenization

A selection of lattice structures has been chosen from two main categories: strut-based lattices and triply periodic minimal surface (TPMS) based lattices. Specifically for this study, the Body-Centred Cubic, Octet-truss, and Schwarz Primitive lattices are used as shown in Table 4. The most important criterion for inclusion in the lattice structure library is manufacturability via AM; therefore, shell-based lattices have not been included due to problems with powder removal [30].

The numerical homogenization routine used in this report is based on the work conducted by Dong et al. [31]. The lattice structure has been

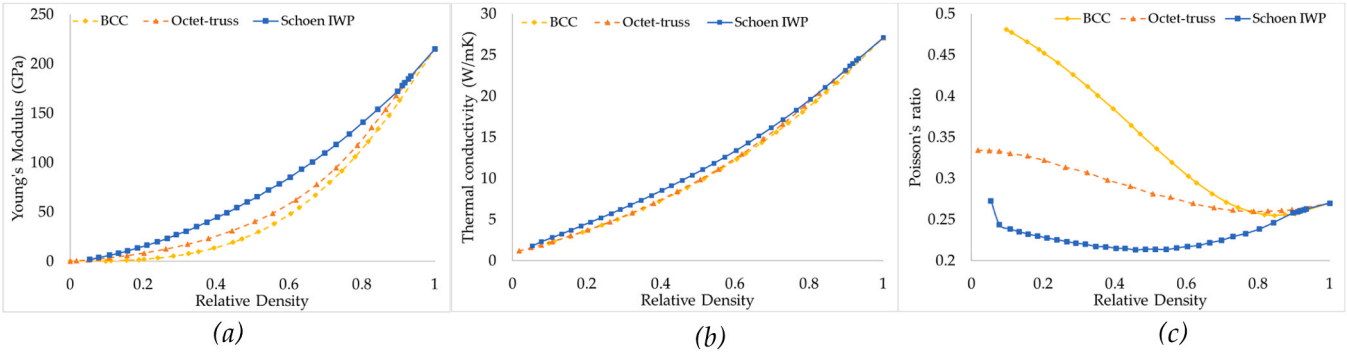

Fig. 8. Material properties as a function of unit density – (a) Young's Modulus (b) Thermal Conductivity (c) Poisson ratio.

Table 5
Homogenized material properties of the selected lattice structures.

	Lattice Density	Young Modulus (GPa)	Thermal conductivity (W/mK)	Poisson's Ratio
BCC	10%	0.626	1.55	0.48
	50%	27.4	9.03	0.34
	80%	113	18.02	0.26
Octet-truss	10%	3.89	2.24	0.33
	50%	38.5	9.74	0.28
	80%	123	19.24	0.26
Schöen-IWP	10%	5.38	2.66	0.24
	50%	62.5	10.77	0.21
	80%	140	19.49	0.24

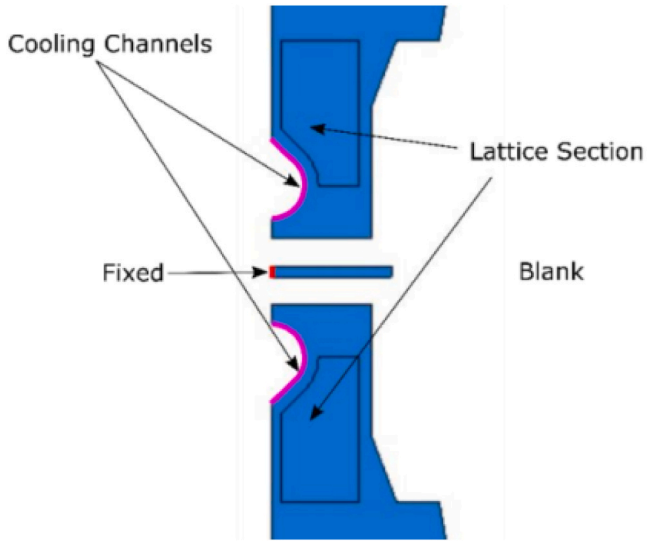

Fig. 9. DoE Simulation Setup.

discretized using a voxel-based approach in which the unit cell is divided into volumetric pixels assigned as either "1", which indicates that the voxel contains material, or "0," which indicates that the voxel does not contain material. For strut-based lattices, the voxel model is generated from a wireframe model by specifying the radius of struts. The minimum length between the voxel's center and the wireframe strut defines whether the voxel is designated as containing material or not. If it is less than the radius of the strut, then the voxel contains material. For TPMS lattices, the process is more straightforward since the surfaces are already mathematically defined. The value of the representative equation is evaluated at the center of each voxel; if this value lies between ± c (the level set constant), then the voxel contains material; otherwise, it does not. The calculated homogenized properties depend on the resolution of the initial voxel model, the resolution meaning the number of voxels along the x, y, and z axes. Using a higher number of voxels is possible to obtain a converged solution. However, at the same time, the computational cost is increased. A sensitivity study was conducted to determine the number of voxels to use, in which the homogenized properties of the Schwartz Primitive lattice structure were calculated for a range of resolutions between 20 and 85 voxels. Based on this study, as shown in Fig. 7, a resolution of 50 was selected, giving an error of less than 0.5% for all calculated properties compared with the converged solution. This represents a compromise between the accuracy of the solution and the computational cost.

Relevant thermo-physical properties of lattices contained within the library, calculated using the described numerical homogenization routine, are shown as a function of relative density in Fig. 8a, Fig. 8b, and Fig. 8c. Both Young's modulus and thermal conductivity follow a Gibson-Ashby relationship. The lattice structure is modelled within the homogenization routine as a composite material comprised of solid material and air. Therefore, at a relative density of 0, Young's modulus of the lattice structure is 0 and the thermal conductivity of the lattice structure is equal to the thermal conductivity of air. At a relative density of 1, all properties are equal to the solid material.

The three types of lattice structures in this study follow the same trend although, for the same relative density, different thermo-mechanical properties are observed. The effective Young's modulus change is due to the lattice mesostructure stiffness variations and regarding thermal conductivity, the variations are caused by differences in the length of the heat path over the unit cell. Overall, it is found that there is a more significant variation in Young's modulus values compared to thermal conductivity values. The change in Poisson's ratio with increasing density is unique for each lattice type. The ability of lattice structures to display variable and even negative Poisson ratios is well documented by Saxena et al. [32].

The homogenized thermo-mechanical properties of the three lattice structures selected for this study are shown in Table 5.

3.3. 2D multi-cycle thermo-mechanical FEA model

The cooling performance of the die designs was assessed using a multi-cycle thermo-mechanically coupled 2D hot stamping simulation developed in ABAQUS. The model consisted of two identical dies containing a single cooling channel and the same model parameters was used as in the validation model and described in Section 3.1. The total length of the die, along the stamping direction, is 45 mm while the length of the working surface is 30 mm. The initial temperature of the dies was set at 25 °C only for the first cycle while for the subsequent cycles, the temperature of the dies is dictated by their temperature at the end of the previous ones. Fig. 9 shows the simulation setup, including information on crucial boundaries and loading conditions. Due to symmetry, only half of the die was directly modelled. The partition in

Table 6
Design of Experiments Results overview.

Die Design	Lattice Type (A)	Lattice Density (B)	Lattice Amount (C)	Channel Radius (D)	Distance to Working Surface (E)	Cooling Rate $CR_{425°C-180°C}$ (°C/s)	Cooling Rate $CR_{450°C-100°C}$ (°C/s)	Stress (MPa)
1	BCC	10%	120°	3 mm	6 mm	527.0	98.0	239.4
2	BCC	50%	180°	4 mm	7 mm	579.4	157.7	104.3
3	BCC	80%	270°	5 mm	8 mm	618.7	183.1	61.9
4	Octet Truss	10%	120°	4 mm	7 mm	552.4	124.8	220.0
5	Octet Truss	50%	180°	5 mm	8 mm	610.5	175.5	91.9
6	Octet Truss	80%	270°	3 mm	6 mm	574.0	155.9	55.0
7	Schöen-IWP	10%	180°	3 mm	8 mm	518.0	113.6	147.5
8	Schöen-IWP	50%	270°	4 mm	6 mm	606.5	173.8	64.0
9	Schöen-IWP	80%	120°	5 mm	7 mm	618.7	179.1	73.7
10	BCC	10%	270°	5 mm	7 mm	613.7	176.3	291.0
11	BCC	50%	120°	3 mm	8 mm	520.0	118.5	97.9
12	BCC	80%	180°	4 mm	6 mm	608.4	174.7	67.9
13	Octet Truss	10%	180°	5 mm	6 mm	562.7	168.3	260.0
14	Octet Truss	50%	270°	3 mm	7 mm	567.6	145.0	71.1
15	Octet Truss	80%	120°	4 mm	8 mm	574.4	158.8	63.7
16	Schöen-IWP	10%	270°	4 mm	8 mm	562.0	150.0	157.5
17	Schöen-IWP	50%	120°	5 mm	6 mm	567.7	168.2	128.4
18	Schöen-IWP	80%	180 °	3 mm	7 mm	578.0	157.4	53.3
Baseline		Solid Die		4 mm	7 mm	608.8	176.3	54.8

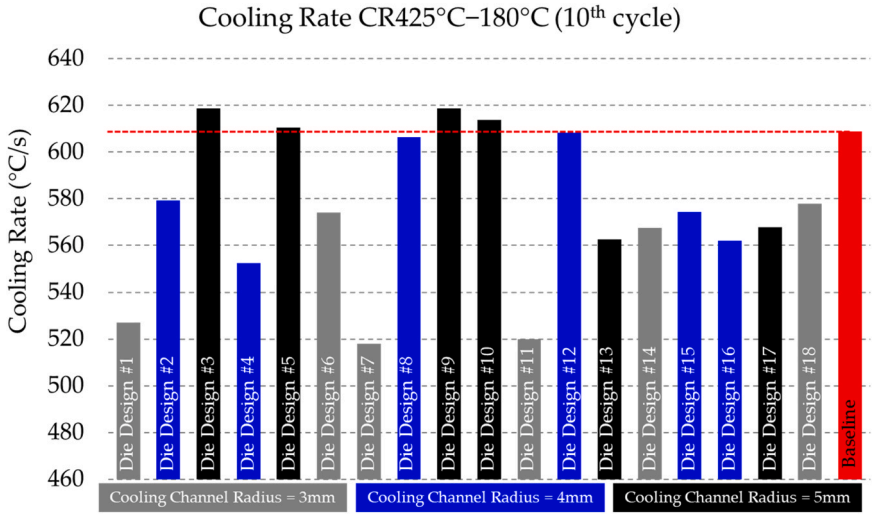

Fig. 10. Results overview for $CR_{425\,°C-180\,°C}$ on the 10th cycle.

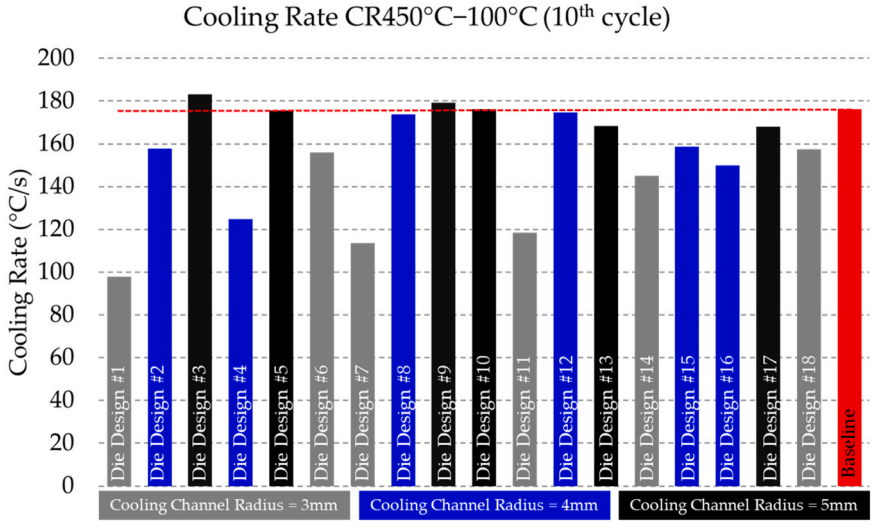

Fig. 11. Results overview for $CR_{450°C-100°C}$ on the 10th cycle.

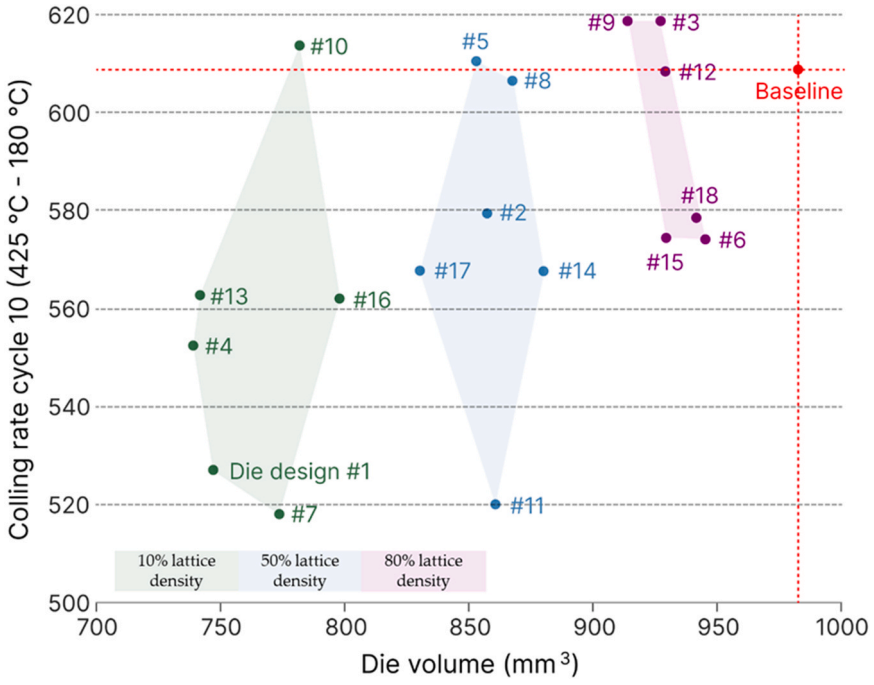

Fig. 12. Die Volume vs $CR_{425\,°C-180\,°C}$.

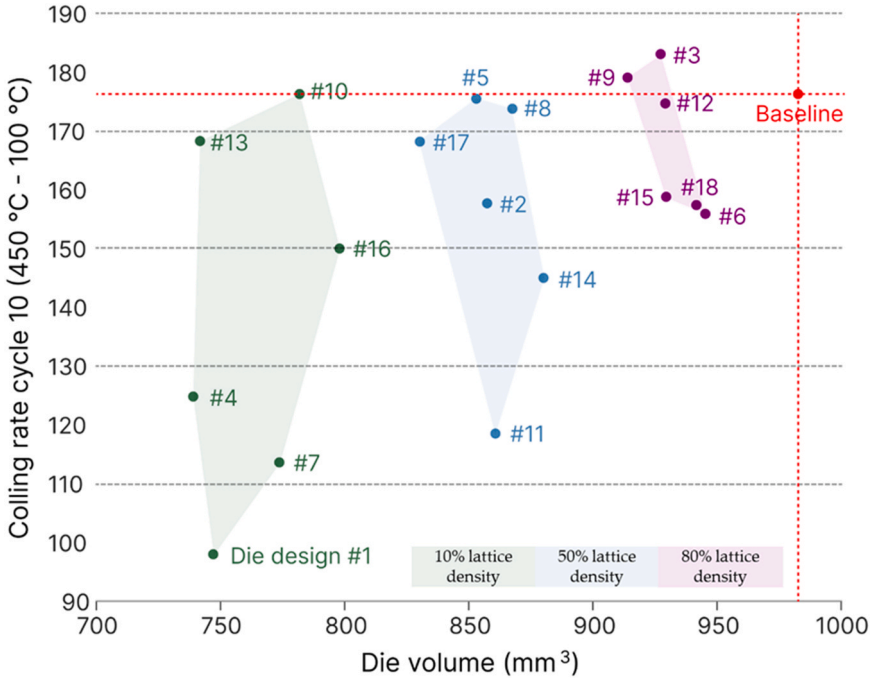

Fig. 13. Die Volume vs $CR_{450°C-100°C}$.

the die face defines the area specified as lattice material where the homogenized material properties of lattice structures are assigned, while the rest of the die has been designated as solid material. In the stamping stage, both the top and bottom die to move at the same speed towards the blank, contacting the surface of the blank for a total of five seconds before returning to their original positions, where they pause for five seconds, emulating a full cycle of hot stamping, including the hot blank loading/positioning, forming and cold die quenching, component unloading and the beginning of the next forming cycle. In total, ten forming cycles were simulated, with the dies assessed according to their cooling performance at the end of the tenth cycle.

4. DoE modeling results

4.1. Results overview

The results of the 18 virtual runs are presented in Table 6, where each run represents a different die design.

It should be noted that while each run consists of 10 hot stamping cycles, the results displayed in Table 6 specifically correspond to the cooling rates observed during the 10th cycle. The values of the two cooling criteria at the 10th cycle, defined in Section 2.3, are presented in Fig. 10 & Fig. 11 while the same data per cycle are presented in Fig. A.1

Table 7
Average and standard deviation of $CR_{425°C-180°C}$ and $CR_{450°C-100°C}$ for different lattice structure integration.

	$CR_{425°C-180°C}$		$CR_{450°C-100°C}$	
	Average	Standard Deviation	Average	Standard Deviation
10% Lattice Density	556.0	33.8	146.6	27.1
50% Lattice Density	575.3	32.9	156.4	21.8
80% Lattice Density	595.5	22.1	168.2	12.2

and Fig. A2.

Both $CR_{425°C-180°C}$ and $CR_{450°C-100°C}$ show a downward trend as the tool temperature increased after several cycles (Fig. A.1 – A2). The baseline cooling trend is represented with a red dotted line. As far as the $CR_{425°C-180°C}$ is concerned, all the dies with a 3 mm cooling channel demonstrate cooling performance lower than the baseline and this fact is attributed to the less circulated water volume in the cooling channel. In the case of a 4 mm cooling channel radius, there is a single case that outperforms the baseline, and the proposed design consists of a θ_{design} angle of 180°, lattice structure density of 80%, and a 6 mm cooling channel distance from the tool-blank interface. However, when the radius of the cooling channel is increased by 1–5 mm, there are 4 cases (Die Design 3, Die Design 5, Die Design 9, and Die Design 10) and the results are presented in Table 6. Die Design 3 and 10 have a θ_{design} angle of 270°, while Die Design 5 and 9 have a θ_{design} angle of 120° and 180°, respectively.

Regarding $CR_{450°C-100°C}$, Die Design 3 and 9 perform better than the baseline, while Dies Design 10 demonstrates similar performance. Finally, the simulated stresses are significantly lower than the yield strength of the tooling material of SS316, and the highest levels are observed in the cases of the strut-based lattices with 10% density. In the case of the Schöen-IWP lattice, which is a TPMS type, and with 10% density, the highest simulated stress is 100 MPa less than in the case of strut-based lattices. This is expected of strut-based lattices because their geometry can act as a site for stress concentration features.

Table 8
Contribution of each design parameter to each response.

Parameter	Cooling Rate (425–180 °C)	Cooling Rate (450 °C −100 °C)	Maximum Stress	Die Volume
Lattice Type (A)	1%	5%	5%	0%
Lattice Density (B)	26%	24%	83%	95%
Lattice Amount (C)	20%	21%	1%	3%
Channel Radius (D)	50%	48%	6%	1%
Distance to Working Surface (E)	3%	2%	4%	1%

4.2. Impact of die volume on cooling rates

To enable a comparison between die designs, a single value is needed to represent the cooling performance of the dies; which is chosen as the stabilised plateau cooling rate or the cooling rate during the tenth cycle. For all investigated die designs, the die volume was plotted against $CR_{425°C-180°C}$ and $CR_{450°C-100°C}$ in Fig. 12 and Fig. 13, respectively. A pattern becomes apparent in the distribution of the relative volumes of the die designs, which is based on the lattice density. All designs with a volume below 800 cm^3 have a lattice density of 10%. Those with a volume between 800 mm^3 and 900 mm^3 have a lattice density of 50% and finally, the dies with a volume above 900 mm^3 have a lattice density of 80%.

There is evidently a connection between die volume and cooling rates, which is caused by the lattice strategy. Table 7 contains the mean and sample standard deviation for the two representative cooling rates

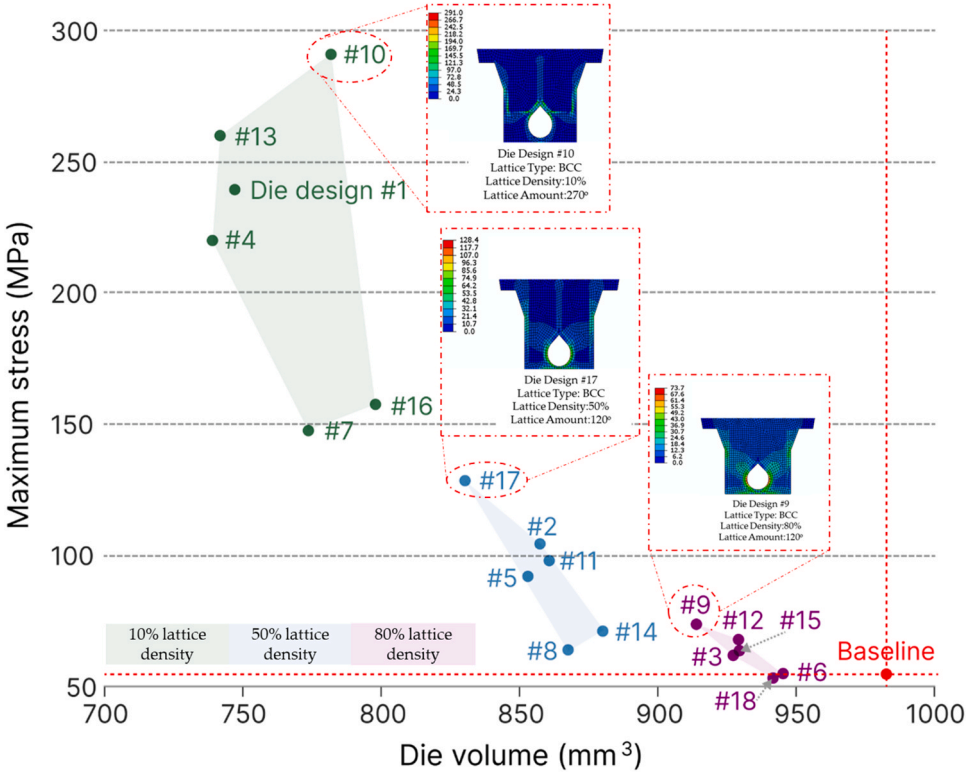

Fig. 14. Die Volume vs Maximum Stress.

Table 9
Outline of specified multi-objective optimization criteria.

	Cooling Rate (425–180 °C)	Cooling Rate (450 °C −100 °C)	Maximum Stress (MPa)	Die Volume (mm^3)
Study #1	Maximize	Maximize	Minimize	Minimize
Study #2	Maximize Weight: 10	Maximize Weight: 8	Target: 50 Upper limit: 200	Target: 800 Upper limit: 900
Study #3	Maximize Weight: 10	Maximize Weight: 8	Minimize	Target: 800 Upper limit: 850

($CR_{425°C–180°C}$ and $CR_{450°C–100°C}$) as separated according to lattice density. It can be observed that the average for both cooling rates increases as the lattice density and, consequently, die volume increases. At the same time, with increased lattice density, the sample standard deviation for both cooling rates decreases, indicating a lower degree of variance in the results. This is expected because lattice structures with lower density act as thermal barriers, exhibiting lower thermal conductivity compared to lattices with higher density, which behave more similarly to fully dense materials. Consequently, the higher the lattice density, the higher the thermal conductivity of the die, thereby enhancing the die's ability to dissipate heat away from the working surface.

This can also be seen in Fig. 12 and Fig. 13, where the data points are more tightly spaced at higher lattice densities. There is also a lower sample standard deviation for $CR_{450\,°C–100\,°C}$, indicating that the lattice strategy has a more significant impact on $CR_{425\,°C–180\,°C}$. However, a lower die volume is not directly correlated with poorer cooling performance; for example, Die Design 11, which has a lattice density of 10%, can achieve a $CR_{425\,°C–180\,°C}$ of 613 °C/s, not significantly lower than the highest observed value of 619 °C/s achieved by Die Design 9, which has a lattice density of 80%.

4.3. Impact of die volume on stress

In Fig. 14, the maximum stress is plotted against the calculated volume for each virtual die. Higher stresses are observed in the cases of dies with lower volumes and especially in the solid-lattice interface as lattice structures act as stress concentration areas. The volume of the die can change either by the different amounts of lattice structure or by their density. The scatter points are color-coded with the brown colour representing 10% of lattice density while the green and the blue 50% and 80% density, respectively. It is observed that a Pareto front is generated, indicating a relation between the level of stresses and the density of the lattice structure. A 10% lattice density comes with a lower die volume but higher maximum stress and, therefore, a poorer load-bearing capacity. The opposite is true for the 80% lattice density, correlated with higher die volume and lower maximum stress. The red dot represents the baseline which is a fully solid die. Although all the DoE runs operate at higher stresses than the baseline, if the yield strength of the die material is considered, it is clear that there is enough flexibility to move toward the top left corner of the scatter plot by selecting a die with lattice structures without compromising the structural integrity of the tool. Thus, the AM of a die can be achieved with lower material costs and reduced printing time.

Table 10
Selected values for each design variable for each study.

	Study #1	Study #2	Study #3
Lattice type	Schöen-IWP	Schöen-IWP	Schöen-IWP
Lattice density	50%	50%	10%
Lattice amount	270°	270°	270°
Cooling channel radius	5 mm	5 mm	5 mm
Distance to the working surface	6 mm	7 mm	7 mm

Table 11
Predicted response variables compared with FEA for Study #1.

	Predicted	F.E. analysis	Error (%)
Maximum Stress (MPa)	101.0	125.7	24%
Cooling rate 450–100 °C (°C s^{-1})	196.3	179.6	9%
Cooling rate 425 °C − 180 °C (°C s^{-1})	613.6	581.8	5%
Volume (mm^3)	860.0	857.8	0%

Table 12
Predicted response variables compared with FEA for Study #2.

	Predicted	F.E. analysis	Error (%)
Maximum Stress (MPa)	100.8	67.5	33%
Cooling rate 450–100 °C (°C s^{-1})	207.1	180.6	13%
Cooling rate 425 °C − 180 °C (°C s^{-1})	624.2	618.9	1%
Volume (mm^3)	868.9	863.4	1%

Table 13
Predicted response variables compared with FEA for Study #3.

	Predicted	F.E. analysis	Error (%)
Maximum Stress (MPa)	227.1	180.1	21%
Cooling rate 450–100 °C (°C s^{-1})	180.3	177.0	2%
Cooling rate 425 °C − 180 °C (°C s^{-1})	608.4	614.3	1%
Volume (mm^3)	774.3	781.8	1%

4.4. Analysis of variance (ANOVA)

The percentage contribution of each factor toward the response variables is outlined in Table 8. These have been calculated according to:

$$P_{C,A} = \frac{SS_A}{SS_T} \times 100 \quad (1)$$

Where $P_{C,A}$ is the percentage contribution of parameter A, SS_A is the sum of squared deviations for control parameter A, and SS_T is the total sum of squared deviations of the total response.

This demonstrates that the most important individual factor contributing to the cooling rates is the cooling channel radius, contributing 50% and 48% towards $CR_{425\,°C–180\,°C}$ and $CR_{450\,°C–100\,°C}$, respectively. However, the contribution of the lattice structure is not insignificant; between the lattice density and lattice amount, 46% and 45% contributions are made towards $CR_{425\,°C–180\,°C}$ and $CR_{450\,°C–100\,°C}$, respectively. The lattice type is not a significant contributor to the cooling performance of the dies, as would be expected since there is not an extensive range in the thermal conductivity of the different lattice types at equivalent densities. Interestingly the distance to the working surface is not indicated as a significant contributor to the cooling performance of the dies, and it may be related to the relatively small range investigated. The lattice density is the most crucial factor in determining both the die volume and the maximum stress. An increasing lattice density acts to improve the structural performance of the die but at the same time increases its volume.

5. Optimization results

Following an analysis of each factor's contribution to the die's overall performance, a general linear model was used to find the optimum combination of design parameters. Three different studies were considered, as outlined in Table 9.

The first study's result is optimized for all response variables, with equal weighting. In the second and third optimization studies, the cooling rate weighting has been increased to 10 for $CR_{425°C–180°C}$, since it is most crucial to the performance of the cooling system, and 8 for

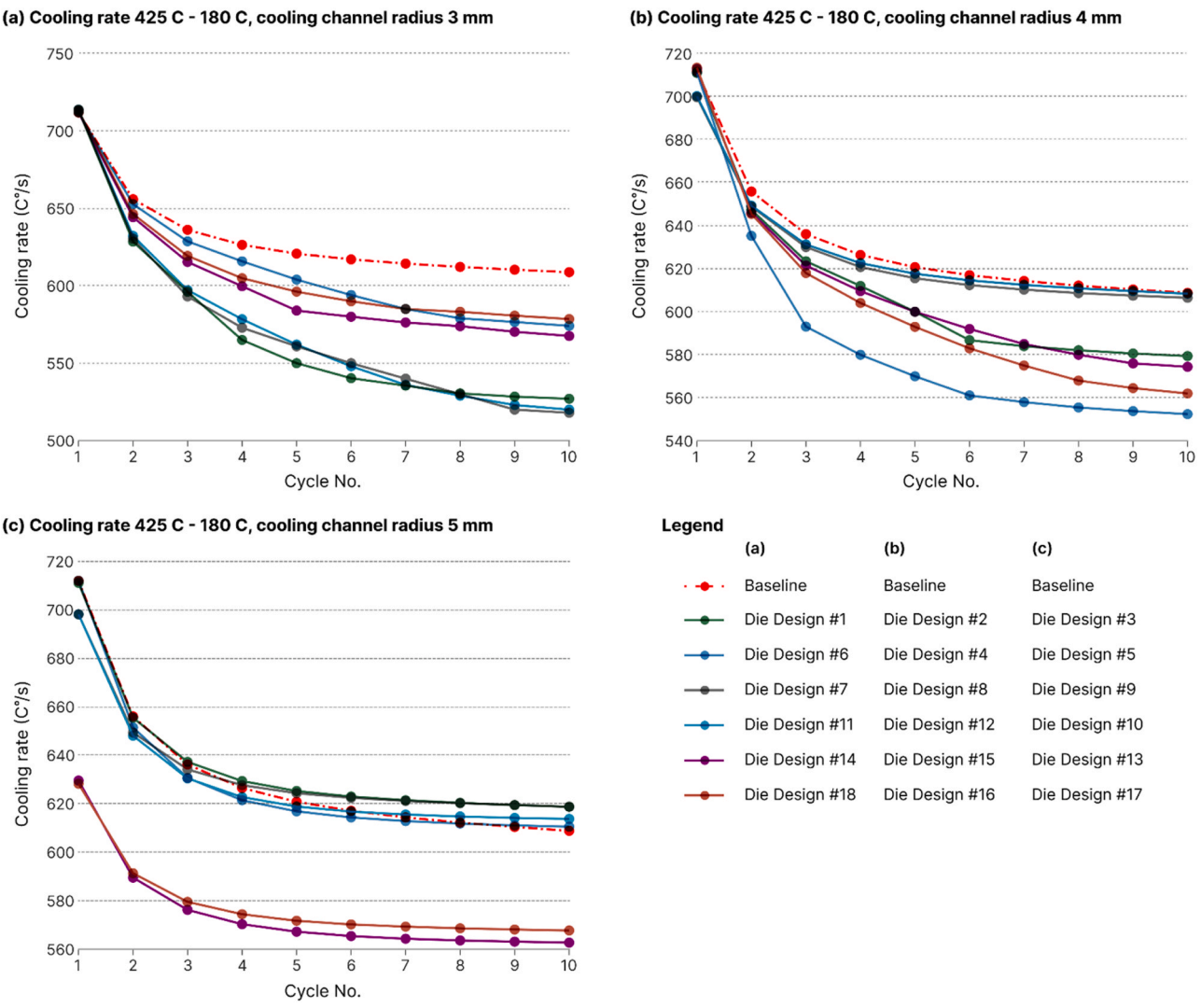

Fig. A.1. Results overview for $CR_{425°C-180°C}$ (a) $CR_{425°C-180°C}$ for die designs with cooling channel radius 3 mm (b) $CR_{425°C-180°C}$ for die designs with cooling channel radius 4 mm (c) $CR_{425°C-180°C}$ for die designs with cooling channel radius 5 mm.

$CR_{450°C-100°C}$. In the second study, the stress response is constrained to an upper limit of 200 MPa, aiming at a target of 50 MPa, while the die volume is constrained to an upper limit of 900 mm^3 with a target of 800 mm^3. In the third study, the constraint on the die volume was relaxed whilst the upper limit on the die volume was reduced to 850 mm^3. The selection of the investigated design parameters for each of the three optimization criteria is outlined in Table 10.

Each study suggests a cooling channel radius of 5 mm as it consistently provides the best cooling performance regardless of lattice strategy. This outcome is expected since the introduction of lattice structures reduces the thermal mass of the die which is effectively compensated for by the increased cooling channel radius. The Schöen-IWP is the lattice structure of choice in all optimization studies as it demonstrates the highest thermal conductivity among the available choices, as it is shown in Fig. 8. Interestingly, as the cooling rate weighting increases, the recommended distance to the working surface changes from 6 mm to 7 mm. This adjustment allows for a larger amount of solid material to be deposited in proximity to the working surface, thereby enhancing the thermal mass of the die and improving its capability to dissipate heat towards the cooling channel. In Study #2, where a more stringent constraint on maximum stress is imposed, a lattice density of 50% is recommended. Conversely, in Study #3, where the stress constraint is relaxed and an emphasis is placed on volume toughness, a lattice density of 10% is suggested. This observation aligns with the expected behaviour, as the reduced amount of material available to withstand mechanical loads leads to higher stresses, thus allowing the algorithm to select of a lattice density of 10%. This reflects the trade-off between the mechanical performance of the die and its material volume.

Three further simulation runs were carried out using the three generated die designs to validate the solutions suggested by the fitted linear model. The F.E. analysis' results were compared with the predictions in terms of the four leading performance indicators. Tables 11–13 show the predicted values of the design response variables compared with the values obtained through F.E. analysis, alongside the percentage error between the two.

The results predicted from the linear model show relatively good agreement with the one generated by FEA for both die volume and critical cooling rates. The best agreement is observed in the die volume, which is expected since there is a linear relationship between the design factors and die volume. In all three studies, for both $CR_{425\,°C-180\,°C}$ and $CR_{450\,°C-100\,°C}$, the predicted values from the linear model are slightly higher than the ones from the FEA model but with the majority having an error of less than 10%. The prediction of the maximum stress experienced by the die is not as good as in the cooling rate case. The error between the linear model and FEA is 21%– 33%. This can be associated with the change of mesh topology, which changes with the change of the

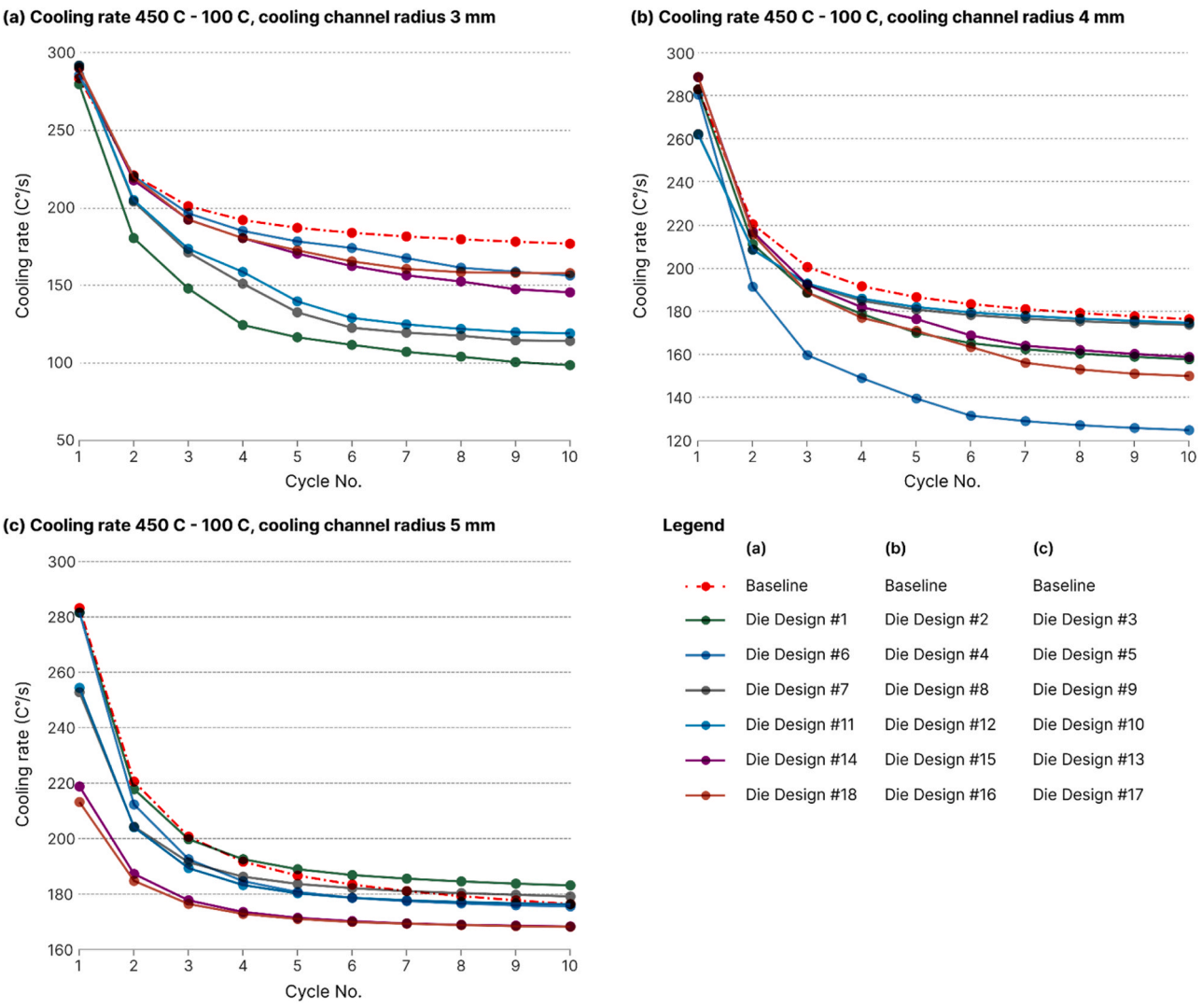

Fig. A.2. (a) $CR_{450°C-100°C}$ for die designs with cooling channel radius 3 mm (b) $CR_{450°C-100°C}$ for die designs with cooling channel radius 4 mm (c) $CR_{450°C-100°C}$ for die designs with cooling channel radius 5 mm.

θ_{design} angle of the system and different nodes experience the maximum stress in each run. However, considering the fidelity of the presented linear model, it can be used to explore the design space in the early stages of developing hot stamping tools.

6. Conclusions

The proposed design of hot stamping tools can provide improved cooling performance, cost and sustainability efficiencies at their manufacturing stage since less material is required. Lattice structures demonstrate reduced thermal conductivity and could be used to efficiently manage the thermal phenomena during and in between hot stamping cycles. However, there is a trade-off between lattice structures and the tools' thermal and mechanical performance. Excessive levels of lattice structures in the die can significantly reduce the tool's load-bearing capability and its capability to handle the thermal loads during quenching. In this study, the basic design parameters of such a die were defined, and a systems engineering approach was used to investigate the impact of these parameters on the system's response. The purpose was to develop and demonstrate a framework in which initial results can be generated quickly to aid in the development of additively manufactured hot stamping tools at the early stage. For this reason, a 2D FEA thermo-mechanically coupled model has been developed, which has been used to simulate a range of lattice integration, following a DoE approach. The proposed framework can be further enhanced by including additional evaluation criteria, such as fatigue or wear, which are both common failure mechanisms of tooling in hot stamping. However, it should be noted that Additive Manufacturing (AM) processes yield anisotropic materials. AMed materials demonstrate porosity, which impacts their thermo-mechanical properties, and achieving a fully dense microstructure is dependent on the specific AM process and the selection of appropriate process parameters. As a common practice, additional post-processing, such as hot isostatic pressing, is often utilized to attain material properties comparable to those of wrought materials [33]. Based on the results, the following conclusions can be made:

- Additively manufactured dies with lattice structures can perform equal to, or better than, a solid die in terms of thermal performance. Although most of the investigated die designs did not perform better than the baseline, some designs in the investigated design space outperformed the baseline. It can be concluded that improved performance can be achieved by increasing the cooling channel radius by 1 mm.
- The optimum design presented in this study consists of a Schoen-IWP lattice, with 50% density, a cooling radius of 5 mm

with 7 mm distance from the working surface, and a θ_{design} angle of 270°. Regarding design variable selection, the results show good agreement with the experimental work on the same topic of Chantzis et al. [25] in which a θ_{design} angle of 270° was found to outperform a solid die. The introduction of lattice structures helps to reduce the thermal mass of the die which will allow it to cool down faster between consecutive cycles. However, as it is observed in this study, there is a "sweet spot" to achieve a better cooling performance as the substitution of large solid areas with lattice structures could potentially hinder the die's cooling performance (Die designs 1,4,7,13 and 14). It is worth mentioning that the solution annealing dwell time for aluminium is usually longer than austenitizing time for steels, which allows the dies to cool down between consecutive cycles. Introducing lattice structures reduces the dies' thermal mass, allowing them to cool down faster between cycles, so they can operate at a lower temperature range, making the quenching more efficient.

- The optimum die design from optimization study 2 in Section 5 has a volume of 868.9 mm^3, where the solid baseline is 982.7 mm^3. The material savings are 11.5%, while the $CR_{425°C–180°C}$ is increased by 3% and $CR_{450°C–100°C}$ by 17%, which shows the sustainability potential of the proposed concept.
- The three design variables associated with the lattice structure and thus with the proposed concept for hot stamping tools have an impact of 50% and 89% on the thermal and mechanical performance, respectively. The proposed design uses a TPMS-type lattice, Schoen-IWP. Although the impact of the lattice type is negligible to the die's thermomechanical performance based on variance analysis, TPMS should be the prime choice due to their ease of manufacture as they are self-supported features.

Author Statement

All persons who meet authorship criteria are listed as authors, and all authors certify that they have participated sufficiently in the work to take public responsibility for the content, including participation in the concept, design, analysis, writing, or revision of the manuscript.

CRediT authorship contribution statement

Dimitrios Chantzis: Writing – original draft, Methodology, Formal analysis, Conceptualization. **Michaela Tracy**: Validation, Formal analysis, Data curation. **Heli Liu**: Writing – review & editing, Validation. **Denis J. Politis:** Writing – review & editing, Supervision. **Mingwang Fu**: Writing – review & editing, Supervision. **Liliang Wang:** Writing – review & editing, Supervision.

Declaration of Competing Interest

The authors declare that they have no known competing financial interests or personal relationships that could have appeared to influence the work reported in this paper.

Data Availability

The data that has been used is confidential.

Appendix – A

See Appendix Fig. A.1 and Fig. A2.

References

[1] European Commission, Zero emission vehicles: first 'Fit for 55' deal will end the sale of new CO2 emitting cars in Europe by 2035,' 2022. ⟨https://ec.europa.eu/commission/presscorner/detail/en/IP_22_6462⟩.

[2] E. Ghassemieh, New Trends and Developments in Automotive Industry, InTech, 2011, https://doi.org/10.5772/1821.

[3] Ducker Worldwide, Unprecedented Growth Expected for Automotive Aluminum as Multi-Material Vehicles Ascend, (2017). ⟨http://www.drivealuminum.org/news-releases/unprecedented-growth-expected-for-automotive-aluminum-as-multi-material-vehicles-ascend-new-survey-of-automakers-says/⟩ (accessed October 16, 2017).

[4] Ducker Worldwide, Aluminum Content in Cars, 2016.

[5] J.N. Hall, J.R. Fekete, Steels for Auto Bodies: A General Overview, Elsevier Ltd, 2017, https://doi.org/10.1016/B978-0-08-100638-2.00002-X.

[6] J. Zhou, B. Wang, J. Lin, L. Fu, W. Ma, Forming defects in aluminum alloy hot stamping of side-door impact beam, Trans. Nonferrous Met. Soc. China 24 (2014) 3611–3620, https://doi.org/10.1016/S1003-6326(14)63506-8.

[7] Z. Wang, P. Liu, Y. Xu, Y. Wang, Y. Zhang, Hot stamping of high strength steel with tailored properties by two methods, Procedia Eng. 81 (2014) 1725–1730, https://doi.org/10.1016/j.proeng.2014.10.221.

[8] N.R. Harrison, S.G. Luckey, Hot stamping of a B-pillar outer from high strength aluminum sheet AA7075, SAE Int. J. Mater. Manuf. 7 (2014), https://doi.org/10.4271/2014-01-0981.

[9] D.W. Fan, H.S. Kim, S. Birosca, B.C. De Cooman, Critical review of hot stamping technology for automotive steels, Mater. Sci. Technol. Conf. Exhib. MS T'07 Explor. Struct. Process. Appl. Across Mult. Mater. Syst. 1 (2007) 98–109.

[10] H. Karbasian, A.E. Tekkaya, A review on hot stamping, J. Mater. Process. Technol. 210 (2010) 2103–2118, https://doi.org/10.1016/j.jmatprotec.2010.07.019.

[11] M. Merklein, M. Wieland, M. Lechner, S. Bruschi, A. Ghiotti, Hot stamping of boron steel sheets with tailored properties: a review, J. Mater. Process. Technol. 228 (2016) 11–24, https://doi.org/10.1016/j.jmatprotec.2015.09.023.

[12] B. Milkereit, M. Österreich, P. Schuster, G. Kirov, Dissolution and precipitation behavior for hot forming of 7021 and 7075 aluminum alloys, Met. (Basel) (2018), https://doi.org/10.3390/met8070531.

[13] B. He, L. Ying, X. Li, P. Hu, Optimal design of longitudinal conformal cooling channels in hot stamping tools, Appl. Therm. Eng. 106 (2016) 1176–1189, https://doi.org/10.1016/j.applthermaleng.2016.06.113.

[14] C. Escher, J.J. Wilzer, Tool steels for hot stamping of high strength automotive body parts, Int. Conf. Stone Concr. Mach. 3 (2015) 219–228.

[15] K. Zheng, C. Tong, Y. Li, J. Lin, Z.C. Kolozsvari, T.A. Dean, An experimental and numerical study of feasibility of a novel technology to manufacture hot stamping dies with pre-constructed tube network, Int. J. Adv. Manuf. Technol. (2020), https://doi.org/10.1007/s00170-020-06280-z.

[16] S. Lee, J. Park, K. Park, D. Kweon, H. Lee, D. Yang, H. Park, J. Kim, A study on the cooling performance of newly developed slice die in the hot press forming process, Met. (Basel) 8 (2018) 947, https://doi.org/10.3390/met8110947.

[17] D. Chantzis, X. Liu, D.J. Politis, O. El Fakir, T.Y. Chua, Z. Shi, L. Wang, Review on additive manufacturing of tooling for hot stamping, Int. J. Adv. Manuf. Technol. 109 (2020) 87–107, https://doi.org/10.1007/s00170-020-05622-1.

[18] J. Chen, P. Gong, Y. Liu, X. Zheng, F. Ren, Optimization of hot stamping cooling system using segmented model, Int. J. Adv. Manuf. Technol. 93 (2017) 1357–1365, https://doi.org/10.1007/s00170-017-0504-x.

[19] L.I.U. Donghao, Die Manufacturing Process-The Best Flow From Idea To Delivery, Politecnico di Torino, 2018. ⟨http://webthesis.biblio.polito.it/id/eprint/7745⟩.

[20] M. Cortina, J. Arrizubieta, A. Calleja, E. Ukar, A. Alberdi, Case study to illustrate the potential of conformal cooling channels for hot stamping dies manufactured using hybrid process of laser metal deposition (LMD) and milling, Met. (Basel) 8 (2018) 102, https://doi.org/10.3390/met8020102.

[21] B. Muller, M. Gebauer, R. Hund, R. Malek, N. Gerth, Metal additive manufacturing for tooling applications - laser beam melting technology increases efficiency of dies and molds, Met. Addit. Manuf. Conf. (2014) 1–14 (Wien), ⟨http://publica.fraunhofer.de/dokumente/N-322053.html⟩.

[22] K.M. Au, K.M. Yu, A scaffolding architecture for conformal cooling design in rapid plastic injection moulding, Int. J. Adv. Manuf. Technol. 34 (2007) 496–515, https://doi.org/10.1007/s00170-006-0628-x.

[23] K.M. Au, K.M. Yu, Modeling of multi-connected porous passageway for mould cooling, CAD Comput. Aided Des. 43 (2011) 989–1000, https://doi.org/10.1016/j.cad.2011.02.007.

[24] H. Brooks, K. Brigden, Design of conformal cooling layers with self-supporting lattices for additively manufactured tooling, Addit. Manuf. 11 (2016) 16–22, https://doi.org/10.1016/j.addma.2016.03.004.

[25] D. Chantzis, X. Liu, D.J. Politis, Z. Shi, L. Wang, Design for additive manufacturing (DfAM) of hot stamping dies with improved cooling performance under cyclic loading conditions, Addit. Manuf. 37 (2021), 101720, https://doi.org/10.1016/j.addma.2020.101720.

[26] S. Kilic, I. Kacar, M. Sahin, F. Ozturk, O. Erdem, Effects of aging temperature, time, and pre-strain on mechanical properties of AA7075, Mater. Res. 22 (2019) 1–13, https://doi.org/10.1590/1980-5373-MR-2019-0006.

[27] SLM Solutions, Fe-Alloy 316L (1.4404) Material Data Sheet, (2021) 1–5. ⟨https://www.slm-solutions.com/fileadmin/Content/Powder/MDS/MDS_Fe-Alloy_316L_0820_V0.91_EN_LS.pdf⟩ (accessed August 31, 2022).

[28] D. Chantzis, X. Liu, D.J. Politis, L. Wang, Additive manufacturing of lattice structured hot stamping dies with improved thermal performance, Phys. Sci. Forum (2022) 25, https://doi.org/10.3390/psf2022004025.

[29] Imperial College Metal Forming Group, Interface Heat Transfer Coefficient of Al7075, (n.d.). ⟨https://smartforming.com/⟩ (accessed June 20, 2022).
[30] T. Maconachie, M. Leary, B. Lozanovski, X. Zhang, M. Qian, O. Faruque, M. Brandt, SLM lattice structures: properties, performance, applications and challenges, Mater. Des. 183 (2019), 108137, https://doi.org/10.1016/j.matdes.2019.108137.
[31] G. Dong, Y. Tang, Y.F. Zhao, A 149 line homogenization code for three-dimensional cellular materials written in MATLAB, J. Eng. Mater. Technol. Trans. ASME 141 (2019), https://doi.org/10.1115/1.4040555.
[32] K.K. Saxena, R. Das, E.P. Calius, Three decades of auxetics research – materials with negative Poisson's ratio: a review, Adv. Eng. Mater. 18 (2016) 1847–1870, https://doi.org/10.1002/adem.201600053.
[33] S.I. Shakil, N.R. Smith, S.P. Yoder, B.E. Ross, D.J. Alvarado, A. Hadadzadeh, M. Haghshenas, Post fabrication thermomechanical processing of additive manufactured metals: a review, J. Manuf. Process. 73 (2022) 757–790, https://doi.org/10.1016/j.jmapro.2021.11.047.